

## PAPER

View Article Online  
View Journal | View Issue



Cite this: *Environ. Sci.: Atmos.*, 2021, 1, 125

## On-road emissions of Euro 6d-TEMP passenger cars on Alpine routes during the winter period†

Ricardo Suarez-Bertoa,<sup>a</sup> Victor Valverde,<sup>a</sup> Jelica Pavlovic,<sup>a</sup> Michaël Clairotte,<sup>a</sup> Tommaso Selleri,<sup>a</sup> Vicente Franco,<sup>b</sup> Zlatko Kregar<sup>b</sup> and Covadonga Astorga<sup>\*a</sup>

The transport sector is an important source of air pollution. Seasonal studies have shown that, in some urban areas, pollution episodes often take place during the cold season. This study investigates how sub-zero ambient temperatures (between  $-8\text{ }^{\circ}\text{C}$  and  $-1\text{ }^{\circ}\text{C}$ ) and high altitudes (from 1300 to 2000 m above sea level) impact the on-road emissions of NO<sub>x</sub>, CO, PN and CO<sub>2</sub> from three Euro 6d-TEMP certified vehicles—one diesel, one gasoline and one plug-in hybrid gasoline–electric vehicle (PHEV). In comparison to tests performed at moderate altitude and ambient temperatures, CO, NO<sub>x</sub> and PN emissions increased under sub-zero temperature, high-altitude conditions for all three vehicles tested. In particular, cold-start emissions from all tested vehicles substantially increase as temperature decreased. Nevertheless, the emissions of NO<sub>x</sub> and PN met the Euro 6d-TEMP on-road emission requirements of the Real Driving Emissions (RDE) test procedure. CO emissions from the diesel and the gasoline vehicles were low. The PHEV had consistently low NO<sub>x</sub> emissions (ranging from 4 to 33 mg km<sup>-1</sup>), but emissions of CO (1010–1849 mg km<sup>-1</sup>) and PN ( $3.5 \times 10^{11}$  to  $1.0 \times 10^{12}$  # per km) were high in some cases. Our results add to the body of evidence indicating that, following the introduction of the RDE in the EU, more efficient emission control technologies are being used to reduce the emissions of NO<sub>x</sub> and PN—the pollutants covered by this test procedure—particularly NO<sub>x</sub> from diesel vehicles. However, the emissions of PN from the two gasoline vehicles were high ( $>1 \times 10^{12}$  # per km) under certain experimental conditions. This result is a reason for concern, because PN emissions from vehicles using the fuel injection technology (PFI, port fuel injection) investigated in this study are not limited by the current Euro 6 regulation. This underlines the need for technology- and fuel-neutral approaches to vehicle emission standards, whereby all vehicles must comply with the same emission limits for the same pollutants regardless of the technologies or fuels employed.

Received 21st October 2020  
Accepted 11th February 2021

DOI: 10.1039/d0ea00010h

rsc.li/esatmospheres

### Environmental significance

Recent seasonal studies have shown that, in some urban areas, a series of air pollutants often related to the transport sector (NO<sub>x</sub>, NH<sub>3</sub>, CO and particulate matter (PM)) reach their highest levels in the cold season. At the same time, laboratory studies have shown that emissions from vehicles increase at cold ambient temperatures. The present study shows that even though cold ambient temperatures negatively impact the emissions from modern gasoline, diesel and plug-in hybrid vehicles, these can meet current emission criteria during real-world operation in the winter season. Moreover, the study shows that the emissions of certain pollutants not regulated by the Euro 6 standard (solid particle number from port-fuel injection vehicles and CO emissions during on-road testing) can be very high in some cases.

## 1. Introduction

Air pollution is a major environmental health burden worldwide, resulting in large economic and environmental impacts.<sup>1</sup> Intense episodes of urban pollution have been clearly associated with the winter season in several studies.<sup>2–4</sup> Recent

seasonal studies have shown that, in some urban areas, the highest levels of NO<sub>x</sub>, NH<sub>3</sub>, CO and particulate matter (PM) occur in the cold season.<sup>5,6</sup> The transport sector is a main source of NO<sub>x</sub>, CO, volatile organic compounds (VOCs), primary aerosols and secondary aerosol precursors in urban areas.<sup>1,7–11</sup> These pollutants play key roles in the formation of tropospheric ozone (O<sub>3</sub>) and secondary aerosols that impair air quality. As a consequence, urban PM composition and in general air quality are strongly influenced by vehicle exhaust emissions.<sup>2,12,13</sup> Vehicles contribute to both the organic and inorganic fraction of the PM via: (i) primary PM emissions and (ii) emissions of precursors of secondary organic aerosols (SOA) and secondary inorganic

<sup>a</sup>European Commission Joint Research Centre, Italy. E-mail: ricardo.suarez-bertoa@ec.europa.eu; covadonga.astorga-llorens@ec.europa.eu

<sup>b</sup>European Commission Directorate-General for Environment, Italy

† Electronic supplementary information (ESI) available. See DOI: 10.1039/d0ea00010h



aerosols, such as VOCs, NO<sub>x</sub> or NH<sub>3</sub>.<sup>7,8,10,14</sup> The tailpipe emissions of these pollutants increase when vehicles are driven at sub-zero temperatures<sup>15–19</sup> as well as at high altitude.<sup>20–22</sup>

The real-driving emissions (RDE) test procedure is an on-road emissions test that is applicable to light-duty vehicles type approvals in the EU [EU 2018/1832].<sup>23</sup> This on-road, real-world test is being used as a model by other regions such as China or India.<sup>24,25</sup> The RDE test procedure accounts for a large variety of real-world driving situations and intends to cover most of the driving situations in Europe, including ambient temperature and altitude profiles. Nonetheless, the RDE procedure excludes some driving situations by setting boundary conditions [EU 2018/1832]. These boundary conditions relate to test duration, ambient temperature, altitude, dynamic driving, positive elevation gain (a measure of uphill driving) and the share of operation by speed ranges (urban/rural/motorway speeds), among others. The measurements may be done at ambient temperatures as low as  $-2\text{ }^{\circ}\text{C}$  for vehicles type-approved as early-stage Euro 6d-TEMP vehicles, and down to  $-7\text{ }^{\circ}\text{C}$  for new passenger car types type-approved after January 2020. Table 1 contains a non-exhaustive list of these requirements and boundary conditions for a test to be RDE-compliant.

The RDE regulation and testing protocol—which was developed across four regulatory packages [EU 2016/427 and EU 2016/646 (both consolidated in EU 2017/1151); EU 2017/1154 and EU 2018/1832]<sup>23,26,27</sup> and a non-binding guidance document<sup>28</sup> introduced “not-to-exceed” (NTE) limits in the type-approval of new vehicles in the EU.† The NTE limits refer to the emissions of NO<sub>x</sub>, and particle number (PN) for all passenger cars and light-commercial vehicles with the exception of PN from non-direct injection gasoline vehicles (*i.e.*, port fuel injection – PFI).

The scope of the present work is to investigate how sub-zero ambient temperatures and high altitudes impact the on-road emissions of NO<sub>x</sub>, CO, PN and CO<sub>2</sub> from three vehicles type-approved under the RDE regulation (all three vehicles type-approved as Euro 6d-TEMP), one diesel, one gasoline and one plug-in hybrid gasoline. To this aim, the overall on-road emissions of the three Euro 6d-TEMP vehicles were comprehensively studied by investigating the combined impact of altitude and temperature on cold-start emissions and their impact on different on-road sections compared to controlled laboratory testing. To do this, all vehicles were tested with a Portable Emissions Measurement System (PEMS) in the Italian Alps during the winter season. Tests were performed along routes not fulfilling the boundary conditions of the RDE procedure described in the Experimental section and then compared to those obtained during ‘baseline’ tests performed in full compliance with the fourth package of the RDE regulation [EU 2018/1832]. Emissions during the urban section of the on-road tests, as well as after cold engine start, were also evaluated due to their particular relevance to urban air quality. Finally, the

vehicles were also tested under controlled conditions at the emissions testing laboratory using the Worldwide Harmonised Light-duty Vehicle Test Procedure (WLTP) at  $-7\text{ }^{\circ}\text{C}$  and  $23\text{ }^{\circ}\text{C}$ .

The results reported in this paper support the development of road transport emission inventory models such as COPERT.<sup>29</sup> Our work also provides values for real-world emissions of pollutants that are not covered by the RDE test procedure currently in force (RDE does not set CO emission limits for any vehicle, nor does the Euro 6 regulation for PN emission limits from non-direct injection gasoline vehicles). Moreover, it presents the first results of vehicles type-approved on-road under the RDE procedure (Euro 6d-TEMP) investigated at sub-zero temperatures and high altitude in real-world driving situations. This offers new information on the emission characteristics of new vehicle types, and provides insights into the emission performance levels that can be expected from them, also under challenging driving situations beyond RDE boundary conditions.

## 2. Experimental

Emissions of NO<sub>x</sub>, CO, PN and CO<sub>2</sub> from one gasoline, one diesel and one gasoline PHEV (vehicle codes GV, DV and PHEV, respectively) were comprehensively studied under different driving conditions on-road and at the Vehicle Emission Laboratory (VELA) of the European Commission Joint Research Centre (JRC) Ispra, Italy. Both gasoline vehicles (GV and PHEV) used port fuel injection (PFI) engines and a three-way catalyst (TWC) as aftertreatment technology. The PHEV was also equipped with an exhaust gas recirculation (EGR) system. The diesel vehicle (DV) was equipped with an EGR, a diesel oxidation catalyst (DOC), a diesel particulate filter (DPF) and a selective catalytic reduction (SCR) system (see Table 2 for main characteristics).

The vehicles were tested by qualified technical staff of the JRC during the 2018 and 2019 winter season. The tests performed for each vehicle included: (i) two RDE-compliant routes (hereinafter RDE1 and RDE2), which act as a baseline, (ii) one route that is close to the maximum altitude boundary of the RDE (1300 meters above sea level) and for which the tests were performed starting at  $-5\text{ }^{\circ}\text{C}$  and  $-4\text{ }^{\circ}\text{C}$  (*i.e.*, below the minimum temperature of  $-2\text{ }^{\circ}\text{C}$  set for Euro 6d-TEMP; hereinafter Alpine1) and (iii) one route that does not fulfill RDE boundary conditions in terms of maximum altitude ( $>2000\text{ m.a.s.l.}$ ), cumulative positive altitude gain ( $>1200\text{ m}/100\text{ km}$ ;  $698\text{ m}$  of positive gain over the first  $9.2\text{ km}$ ; see Fig. 1), and for which minimum test temperatures were between  $-8\text{ }^{\circ}\text{C}$  and  $-1\text{ }^{\circ}\text{C}$  (hereinafter Alpine2 (extra)). Table 3 summarizes the main features of the routes used and Table S1 of the ESI† summarizes the number of test repetitions for each route and vehicle. Fig. 1 illustrates the altitude profile of the different routes.

The measurement of the instantaneous on-road emissions of NO<sub>x</sub>, CO, PN and CO<sub>2</sub> was performed using a PEMS. Vehicles were tested using an AVL MOVE system (AVL, Graz, Austria – model 2016). The PEMS used consists of a tailpipe attachment, heated exhaust sampling lines, an exhaust flow meter (EFM), exhaust gas analyzers, a data logger connected to the vehicle

† During RDE phasing-in (2017–2019) a temporary conformity factor of 2.1 for NO<sub>x</sub> tailpipe emissions may apply upon the request of the manufacturer. Vehicles type-approved under this requirement fall under the Euro 6d-TEMP standard.



**Table 1** Non-exhaustive list of the requirements and boundary conditions for a test to be RDE compliant

Altitude	Moderate conditions	0–700 m.a.s.l.
	Extended conditions	700–1300 m.a.s.l.
Ambient temperature	Moderate conditions	0–30 °C
	Extended conditions	–7–0 °C and 30–35 °C
Cumulative positive altitude gain		1200 m every 100 km
Altitude difference between start and finish		<100 m
Dynamics	Upper limits	95 <sup>th</sup> percentile of the multiplication of the instant speed and positive acceleration signals as defined in Appendix 7a, Section 4 of RDE 4
	Lower limits	Relates to the relative positive acceleration as defined in Appendix 7a, Section 4 of RDE 4
Maximum speed		145 km h <sup>–1</sup> (up to 160 km h <sup>–1</sup> for <3% of motorway driving time)
Payload		Maximum 90% of the maximum vehicle weight (including the mass of the driver and measurement equipment)
Stop percentage		Between 6% and 30% of the urban driving time
Speed	Average urban speed	15–40 km h <sup>–1</sup>
Distance		Above 100 km h <sup>–1</sup> for at least 5 minutes
Trip composition		Urban >16 km; rural >16 km; motorway >16 km
		Urban 29–44% of the total distance; rural 23–43% of the total distance; motorway 23–43% of the total distance
Total trip duration		90–120 minutes
Use of auxiliary systems		Operated as in real life use (air conditioning, etc.)

**Table 2** Vehicle specifications<sup>a</sup>

Code	GV	DV	PHEV
Make	Citroën	Peugeot	Mitsubishi
Model	C3	308	Outlander
Fuel	Gasoline	Diesel	Gasoline
Injection	PFI	DI	PFI
Emission control system	TWC	DOC + EGR + DPF + SCR	TWC + EGR
Registration	2018	2018	2018
Mileage (km)	939	9680	541
Euro standard	Euro 6d-TEMP	Euro 6d-TEMP	Euro 6d-TEMP
Engine capacity (cm <sup>3</sup> )	1199	1499	2360
ICE power (kW)	61	96	99

<sup>a</sup> PFI (port fuel injection); DI (direct injection); TWC (three-way catalyst); DOC (diesel oxidation catalyst); EGR (exhaust gas recirculation); DPF (diesel particulate filter); SCR (selective catalyst reduction system); ICE (internal combustion engine).

engine control unit, a GPS and a weather station for ambient temperature and humidity measurements. The system measures exhaust gas concentrations of CO and CO<sub>2</sub> by a non-dispersive infrared sensor, and NO<sub>x</sub> by a non-dispersive ultra-violet sensor. Emissions of solid particle number (PN) with a particle diameter cut-off of 23 nm were measured by means of the diffusion charger principle. The EFM uses a pitot tube to estimate the exhaust mass flow rate. All relevant emissions data were recorded at a frequency of 1 Hz. The gases and PN

analyzers were all kept inside the vehicles and connected to the mains during the soaking period.

Duplicate tests were performed with vehicles DV and GV in the test cell at 23 °C and –7 °C applying the WLTP. The vehicle PHEV was tested once at each temperature – see Table S1 of the ESI.<sup>†</sup> The laboratory tests were performed in a climatic test cell with controlled temperature and relative humidity to simulate ambient conditions, equipped with a chassis dynamometer designed for two and four-wheel drive light-duty vehicles. Gaseous emissions were measured using non-dispersive infrared (for CO/CO<sub>2</sub>), a chemiluminescence detector (for NO<sub>x</sub>) and a heated (191 °C) flame ionization detector (FID; for THC). A solid particle number measurement system (AVL APC 489), with a particle diameter cut-off ( $d_{50\%}$ ) of 23 nm, compliant with the light-duty vehicles Regulation 83 (ref. 30) was used at the CVS to measure PN emissions. Emission factors were calculated as described in the WLTP regulation [EU 2017/1151] without the application of regeneration factors, RCB and ATCT corrections. For vehicle PHEV, utility factor weighted emission factors are provided. These are calculated as indicated in the WLTP for plug-in hybrid-electric vehicles (also referred to as off-vehicle charging hybrid electric vehicles or OVC-HEV), and include weighed emissions considering the test where the battery is fully charged (charge-depleting mode) and the emissions of the cold-start test performed with the depleted battery (charge-sustaining mode). For more details, see Global Technical Regulation (GTR) No. 15 (ref. 31) and Suarez-Bertoa *et al.*<sup>32</sup>

The on-road emission factors reported in this paper were calculated by integrating the total mass emissions measured



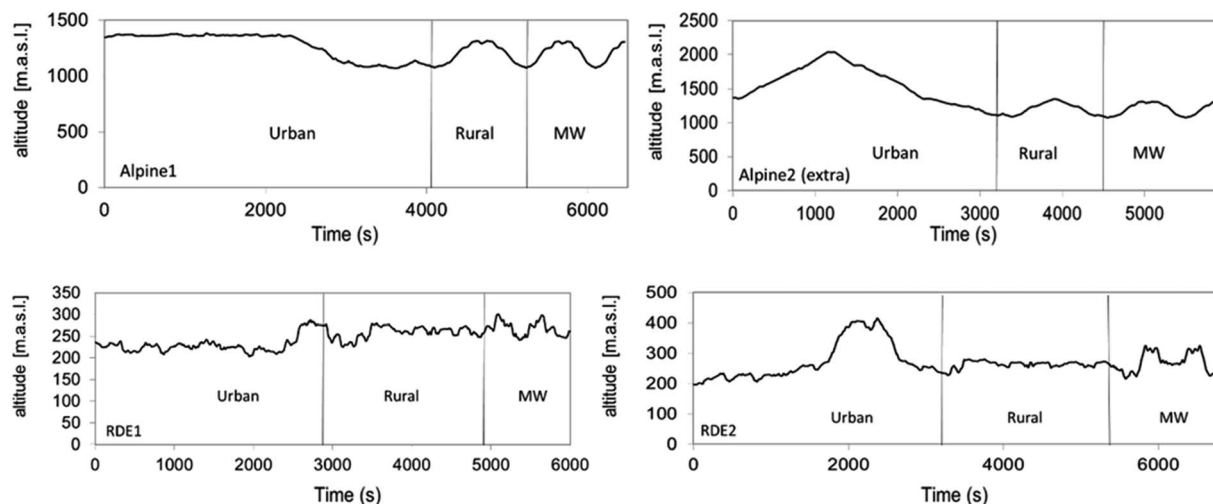


Fig. 1 Altitude profiles of the tested routes: route Alpine1 (top-left), route Alpine2 (extra) (top-right), route RDE-1 (bottom-left), and route RDE-2 (bottom-right).

Table 3 Trips characteristics. Bold indicates that the value is outside RDE boundary conditions

	RDE1	RDE2	Alpine1	Alpine2 (extra)
Trip distance (km)	79	94	87	84
Average trip duration (min)	94	112	108	91
Average urban distance (km)	31	37	36	36
Average rural distance (km)	25	27	24	22
Average motorway distance (km)	23	30	27	25
Urban average speed (km h <sup>-1</sup> )	29	29	29	37
Cumulative positive gain (m/100 km)	760	820	1015	<b>1687</b>
Max trip altitude (m.a.s.l.)	300	415	1380	<b>2040</b>
Coolant <i>T</i> (°C) at <i>t</i> = 0 s	DV 23 GV 13 PHEV 8	23 13 —	−2 & 4 −1 & 3 4	0 & 3 −2 & 4 6

during the test and dividing the obtained value by the driven distance, as estimated from the GPS velocity signal. These are the so-called ‘raw’ emissions factors (without using the weighting function based on CO<sub>2</sub> emissions as introduced by the fourth package of the RDE regulation) [EU 2018/1832; Annex VI] and without applying the 1.6 correction coefficient for extended conditions. The urban emission factors during the on-road tests correspond to the emissions during the urban section as defined in Annex IIIA of the RDE regulation (*i.e.*, when vehicle speed <60 km h<sup>-1</sup>). The urban emission factors from the WLTP test are those measured during the low phase (phase 1) of the worldwide light duty test cycle-WLTC, which covers the first 3.1 km of the cycle. The emission factors of the so-called ‘cold-start’ were calculated considering the emissions from the first 300 seconds following the first time the internal combustion engine (ICE) ignites, divided by the distance driven in that period. This approach was used for the on-road and the laboratory tests. In the RDE regulation the

cold-start is considered to finish when the coolant temperature reaches 70 °C, or 300 s after the first ignition of the ICE, whichever comes first. In our tests, the elapsed time condition was always met first.

During the Alpine test campaign, the vehicles were soaked at a temperature that ranged from −8 °C to −1 °C for 8–12 hours. Nonetheless, the coolant temperatures of the vehicles at the moment the test started ranged from −2 °C to 6 °C (Table 3). The initial coolant temperature of the vehicles during WLTP tests was equal to the test cell set temperature, *i.e.*, 23 °C or −7 °C. During the RDE-compliant tests vehicles DV, GV and PHEV were soaked for 14–17 hours. For these tests, DV was soaked at 23 °C, and GV and PHEV were soaked at 13 °C and 8 °C.

Vehicles DV and GV were tested with the air heating system activated along all routes. The vehicle PHEV was tested along the routes Alpine1 and Alpine2 (extra) with the air heating system enabled and disabled (set in automatic mode at 21 °C when on; hereinafter, Heat-ON and Heat-OFF, respectively) and using two different initial battery states of charge (SOCs), 100% and depleted battery or battery under charge sustaining conditions (hereinafter SOC-min). Studying the vehicle in different modes allowed us to explore how it managed the use of the ICE and the electric motors under these ambient and road conditions and the resulting effect on emissions. For the PHEV, only the RDE1 route was driven (for testing configurations see Table S1 of the ESI†).

The exhaust flow meter experienced an offset during the test on the Alpine1 route using the SOC-min and Heat-OFF setup of the PHEV. In order to have a rough estimation of the emission factors, the shift was corrected by a constant multiplicative factor of 3.7 (see Fig. S1 of the ESI†). This offset correction was obtained by comparison with the test Alpine1 route using the SOC-min and Heat-ON setup. During the motorway operation, when the ICE is used, the two tests should provide similar exhaust flow. This is also reflected for the tests performed on the same route with SOC 100% (see Fig. S1 of the ESI†).





### 3. Results and discussion

Fig. 2, 3 and Table S2 of the ESI† summarize NO<sub>x</sub>, PN, CO and CO<sub>2</sub> emission factors from the three vehicles. They include the results obtained for the complete tests, the urban section and the cold-start of the tests performed using the four different routes and during the WLTP at 23 and −7 °C. The PHEV's emission factors correspond to tests at 100% battery SOC and with the heating system enabled (Heat-ON). Fig. 4 illustrates the emissions of NO<sub>x</sub>, PN and CO from all three vehicles during the on-road tests (Alpine1, Alpine2 (extra) and RDE). The emission factors are presented for the entire on-road tests (total) and their sub-sections (*i.e.*, urban, rural and motorway sections) as a function of their corresponding average speed (see also Table S3 of the ESI†).

Due to the uncontrolled nature of some of its elements, RDE testing is non-replicable. Even when vehicles are tested on the

same route, testing conditions (including but not limited to traffic, temperature, and driving dynamics) may be different. These different testing conditions may result in different emissions. Hence, RDE tests are not meant for direct comparisons, but rather to ensure that pollutant emissions are well controlled under a broad range of driving conditions. The discussion on on-road CO<sub>2</sub> emissions presented here is therefore of qualitative nature and corresponds to conditions well beyond the boundaries of the type-approval WLTP test.

#### 3.1. Emissions from the Euro 6d-TEMP diesel vehicle (DV)

Emissions of CO, NO<sub>x</sub> and PN from the DV were higher at colder temperatures during both laboratory and on-road tests (Fig. 2 and Table S2 of the ESI†) than at 23 °C or under moderate ambient conditions. NO<sub>x</sub> raw emissions during every single on-road test were always below the Euro 6d-TEMP on-road emission requirement ( $80 \text{ mg km}^{-1} \times 2.1$  conformity factor), for the complete tests and the urban sections (with the exception of the NO<sub>x</sub> urban emission factor,  $178 \text{ mg km}^{-1}$ , during one of the two Alpine2 (extra) tests performed). The highest NO<sub>x</sub> emissions factors on the road ( $113 \pm 4 \text{ mg km}^{-1}$ , expressed as the average of recorded values  $\pm$  standard deviation of two tests) were obtained during the Alpine2 test (extra), which was the most demanding test in terms of road grade, altitude and cold ambient temperature. From Fig. S2 of the ESI†, it is evident how most of the NO<sub>x</sub> emissions were produced after the initial climb and after cold start, possibly due to the effect of the long period of downhill driving at low ambient temperatures which might have hindered the proper function of the SCR unit. However, the highest NO<sub>x</sub> emissions factor resulted from the Low-T WLTP (Fig. 3), which, under these controlled conditions was  $\sim 3.6$  times higher than that at 23 °C. When analyzed together, these two elements suggest that: (i) cold ambient temperature has a strong negative impact on NO<sub>x</sub> emissions from diesel vehicles; (ii) the distance of the test plays an important role when calculating emission factors (mass/distance units), particularly if the pollutants are mainly emitted during cold-start.

Grange *et al.*<sup>44</sup> have recently shown, using remote sensing techniques, that light-duty diesel NO<sub>x</sub> emissions are highly dependent on ambient temperature with low temperatures resulting in higher NO<sub>x</sub> emissions. In particular, for pre-RDE Euro 6 vehicles they indicated that LNT equipped vehicles have a stronger temperature dependence than SCR equipped vehicles. The study anticipated that manufacturers would have to implement SCR technology to ensure compliance with the European NO<sub>x</sub> emission limits during real driving emission (RDE) tests. Recent laboratory studies<sup>15,17,32</sup> reported a systematic increase of NO<sub>x</sub> emissions from Euro 6b diesel vehicles equipped with SCR systems, when tested at −7 °C compared to 23 °C under the WLTP (from  $150\text{--}609 \text{ mg km}^{-1}$  at 23 °C to  $390\text{--}1417 \text{ mg km}^{-1}$  at −7 °C). The higher NO<sub>x</sub> emissions were explained by lower EGR operation and lower SCR efficiency at −7 °C compared to 23 °C. Vehicle DV (Euro 6d-TEMP) emitted  $65 \pm 2 \text{ mg km}^{-1}$  at 23 °C and  $233 \pm 19 \text{ mg km}^{-1}$  at −7 °C, which indicates a substantial improvement

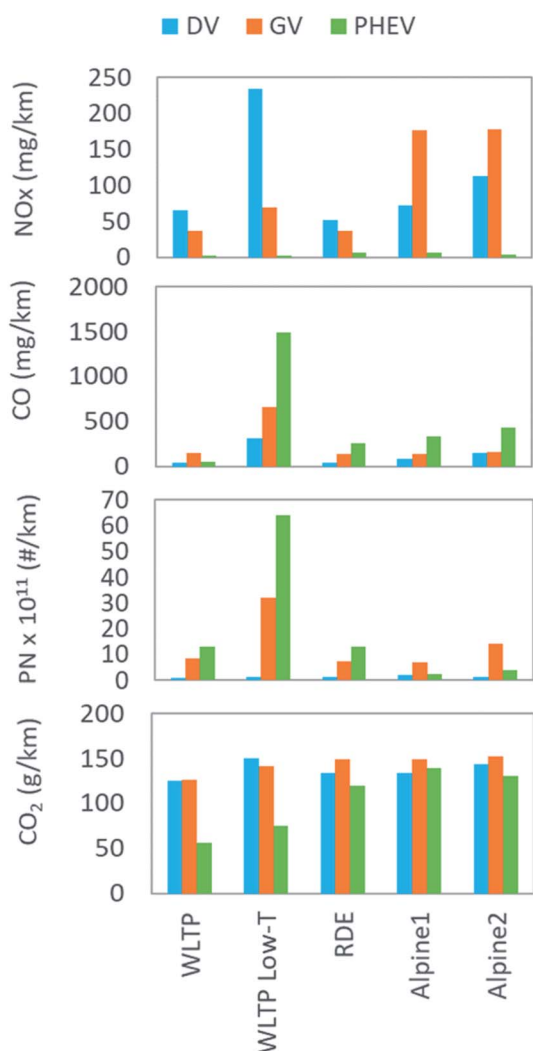


Fig. 2 Emission factors of NO<sub>x</sub>, PN, CO and CO<sub>2</sub> from DV (blue), GV (orange) and PHEV (green) during the entire routes Alpine1, Alpine2 (extra) and RDE as well as during the laboratory tests over the WLTP at 23 °C and −7 °C. The PHEV's emission factors correspond to tests at 100% SOC with the air heating system on.



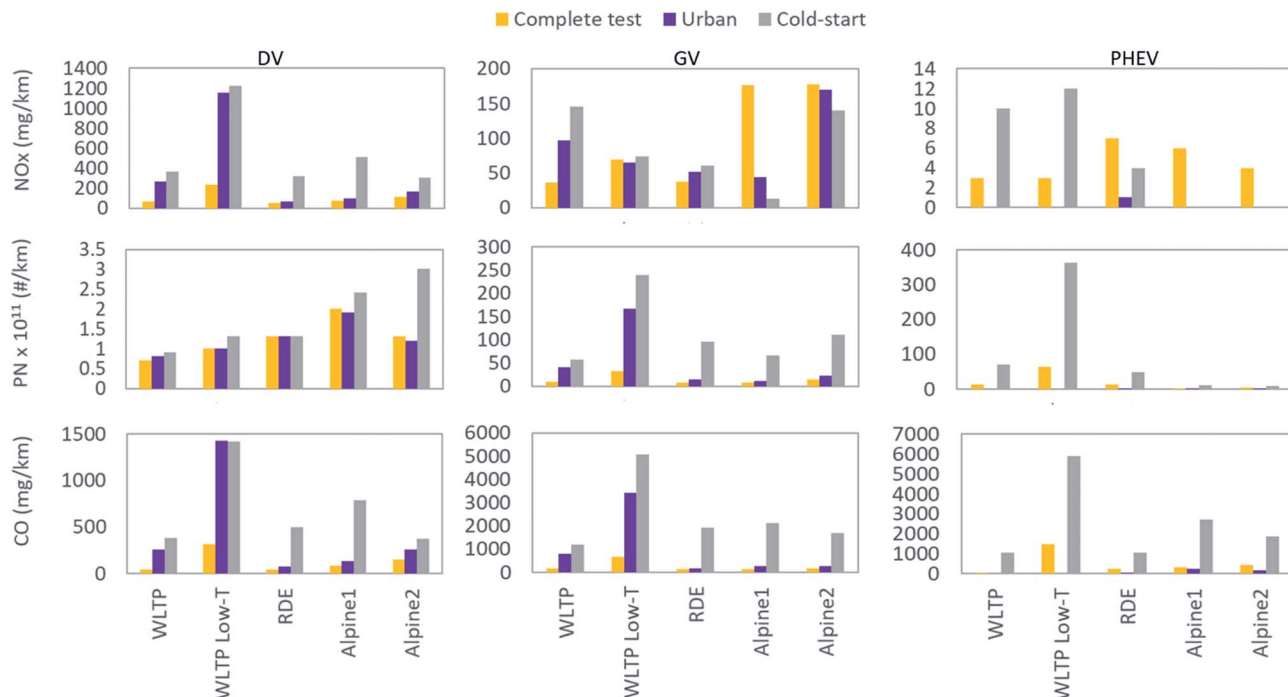


Fig. 3 Emission factors of NO<sub>x</sub>, PN, CO and CO<sub>2</sub> from DV, GV and PHEV during the entire on road (RDE, Alpine1 and Alpine2 (extra)) and laboratory (WLTP) tests (yellow bars), the urban section of the on-road tests and the phase 1 of the WLTP (violet bars) and the cold-start (grey bars).

compared to the Euro 6b (pre-RDE) diesel vehicles tested in previous studies.

NO<sub>x</sub> emissions from the DV during the Alpine tests ( $72 \pm 1$  mg km<sup>-1</sup> for Alpine1 and  $113 \pm 4$  mg km<sup>-1</sup> for the route Alpine2 (extra)) were up to two times higher than those measured during the RDE-compliant route tests ( $51 \pm 29$  mg km<sup>-1</sup>) performed at 24 °C. In absolute numbers, the increase in NO<sub>x</sub> emissions from the DV is lower than that reported by Wang *et al.*<sup>20</sup> for a series of tests performed with a China IV diesel vehicles at different altitudes but similar ambient temperature ( $\sim 580$  mg km<sup>-1</sup> at 30 m.a.s.l.,  $\sim 740$  mg km<sup>-1</sup> at 1330 m.a.s.l. and  $\sim 760$  mg km<sup>-1</sup> at 1910 m.a.s.l.). The rise of NO<sub>x</sub> emissions under these ambient conditions could be related to the operation of the exhaust gas recirculation (EGR) valve. The vehicle's engine control unit (ECU) could close the EGR valve to maintain the combustion process when pressure gets lower at higher altitudes, or when temperature decreases below zero.<sup>33</sup> This would lead to the formation of NO<sub>x</sub>. It could also be related to the increased time needed by the SCR to reach the optimal operating temperature,<sup>34</sup> to the difficulty of maintaining a suitable operative temperature under cold ambient conditions or to the cumulative altitude over the urban phase of the Alpine2 (extra) trip compared to Alpine1 and RDE tests. From the inspection of Fig. S2 of the ESI,<sup>†</sup> it seems that cold-start emissions are comparable in the three cases, suggesting that the latter hypothesis might be more reasonable.

While urban NO<sub>x</sub> emission accounted for 54–63% (Fig. 5) of the total emissions ranging from  $67 \pm 45$  mg km<sup>-1</sup> on the RDE-routes to  $169 \pm 14$  mg km<sup>-1</sup> on the Alpine2 route (extra)

(Fig. 4a), motorway NO<sub>x</sub> emissions were comparable for all the tests performed on the road (see Table S3 of the ESI<sup>†</sup>). This suggests that once the SCR system reaches its operating temperature and the vehicle is driven at higher loads NO<sub>x</sub> emissions are controlled independently of the ambient temperature and altitude.

Cold-start emission factors are an important indicator of the contribution of passenger car emissions to the urban areas.<sup>35</sup> They have recently been considered to have become one of the main sources of pollutants on Euro 6d-TEMP cars.<sup>36</sup> Hence, using cold-start emission factors in urban air quality models may be more representative of the real contribution of the passenger car sector in cities. Using the time condition to define cold-start (300 seconds) described in the RDE regulation, our cold-start period was  $\sim 2$ –3 km for most of the tests performed (see Table S2 of the ESI<sup>†</sup>). Although cold-start NO<sub>x</sub> emissions only accounted for 8–15% of the total NO<sub>x</sub> emissions of the on-road tests, cold-start NO<sub>x</sub> emission factors are higher than NO<sub>x</sub> emission factors for the urban section and the whole test (see Fig. 5 and Table S2 of the ESI<sup>†</sup>). Cold-start NO<sub>x</sub> emissions from the Alpine1 route were 1.6 times higher than those from RDE-routes ( $323 \pm 15$  mg km<sup>-1</sup>). However, during the Alpine2 test (extra) (performed at  $-7$  °C and with a high positive road grade) they were comparable (within uncertainties) to those measured on the RDE-routes (performed at 24 °C and with little positive road grade). The high positive road grade of the Alpine2 route (extra) may have helped warming up faster the aftertreatment system, improving its NO<sub>x</sub> control efficiency.



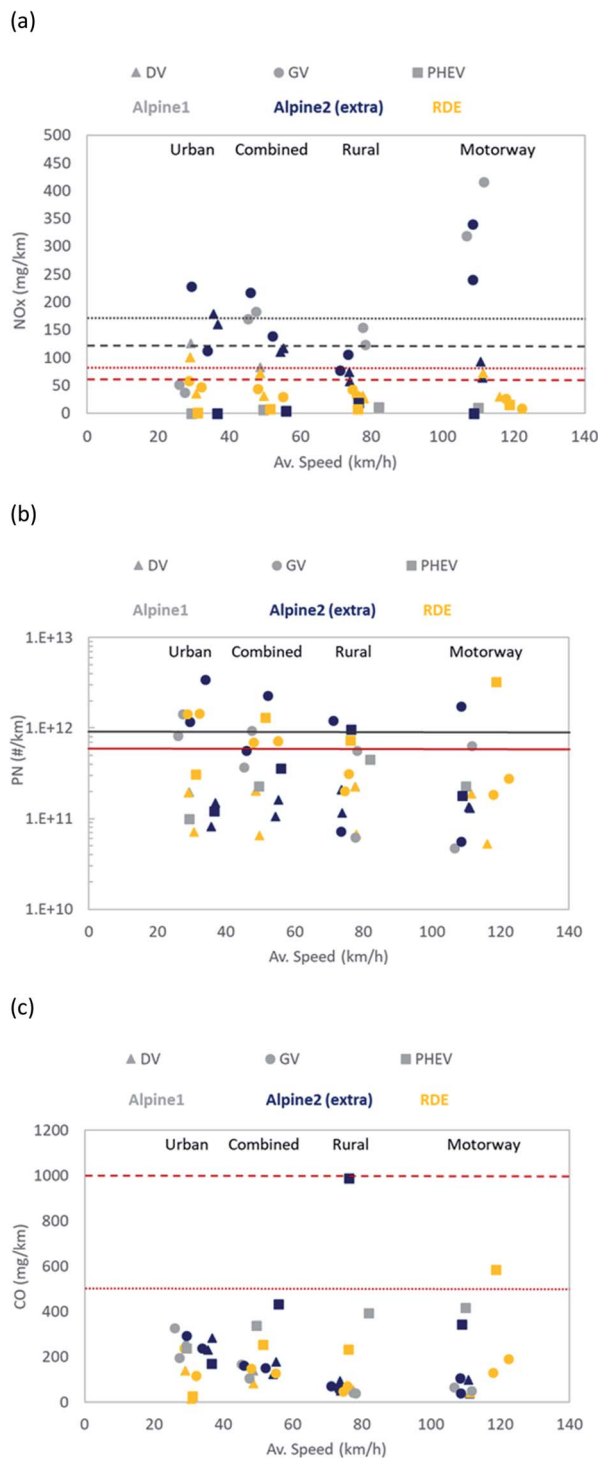


**Fig. 4** Emission factors of (a) NO<sub>x</sub>, (b) PN and (c) CO from DV (triangles), GV (circles) and PHEV (squares) as a function of vehicle average speed on the entire Alpine1 (grey), Alpine2 (extra) (blue) and RDE routes (yellow). The emission factors are presented for the entire tests (combined) and their sub-sections (urban, rural and motorway). The PHEV's emission factors correspond to tests at 100% SOC with the air heating system on. For illustrative purposes, red lines indicate Euro 6 regulatory limits; grey lines indicate Euro 6d-TEMP NTE limits (only applicable for NO<sub>x</sub> and PN results from urban and complete phases over the RDE compliant test and calculated according to the RDE4 regulation); dashed lines apply to gasoline vehicles; dotted lines apply to diesel vehicles; solid lines are only used for PN and apply to both diesel and direct injection gasoline vehicles.

Although cold temperature and high altitude negatively affected NO<sub>x</sub> emissions during the complete on-road tests and their urban section, they did not seem to have a strong impact on the cold-start NO<sub>x</sub> emissions of vehicle DV for the tests where the initial coolant temperature was between 0 °C and 23 °C. However, during the WLTP tests where it was at −7 °C, also for the on-road test performed along Alpine1 with the initial coolant temperature at −2 °C, the NO<sub>x</sub> emissions were strongly affected and presented the highest values measured for this vehicle (see Fig. 6 and Table S2 of the ESI†). Hence, the colder the vehicle and its components (engine and after-treatment systems) are, the higher the NO<sub>x</sub> emissions.

PN emissions from vehicle DV were higher during the cold ambient and high altitude tests than during the other tests performed. Nonetheless, they were relatively low, and consistently below the NTE and even the Euro 6 regulatory limit of  $6 \times 10^{11}$  # per km, during all the tests performed, which demonstrates a sufficiently good performance of the DPF. PN emission factors ranged from  $1 \times 10^{11}$  # per km on the RDE compliant routes to  $2 \times 10^{11}$  # per km on the Alpine1 route. PN emission factors were slightly elevated during the urban sections and cold-start (up to  $5 \times 10^{11}$  # per km). PN emissions at cold-start were also below  $6 \times 10^{11}$  # per km showing good control of the emissions by the DPF. It should be noted that there was no DPF regeneration recorded during the performed tests.

Compared to its laboratory regulatory limit (Euro 6 limit for light-duty diesel vehicles over the WLTP at 23 °C is  $500 \text{ mg km}^{-1}$ ), CO emissions measured from vehicle DV were relatively low during all the on-road tests and the WLTP at 23 °C. The highest CO emissions during the complete tests were measured during the WLTP at −7 °C ( $318 \pm 61 \text{ mg km}^{-1}$ ). The urban section accounted for the largest part of the CO emissions (60–80%). CO emission factors ranged from  $74 \pm 74 \text{ mg km}^{-1}$  (RDE-routes) to  $1428 \pm 630 \text{ mg km}^{-1}$  (WLTP at −7 °C). Emission factors for cold-start were also substantially higher than urban emission factors for the on-road tests, ranging from  $497 \pm 304 \text{ mg km}^{-1}$  (RDE-routes) to  $789 \pm 334 \text{ mg km}^{-1}$  (Alpine1 route). The CO emissions of the vehicle DV during the Alpine1 and Alpine2 (extra) tests were in line with those reported for Euro 6b diesel vehicles tested at −7 °C over the WLTP<sup>17,32</sup> but five times lower than those reported by Weber *et al.* at the same temperature over the NEDC.<sup>15</sup>

Although Wang *et al.*<sup>20</sup> reported higher emissions of CO and PN at higher altitudes for a China IV-certified diesel vehicle tested on-road from 30 to 2990 m.a.s.l., those measured for the DV were low and comparable under both conditions. This is in line with previous studies that have shown that PN and CO emissions from modern diesel vehicles are only slightly affected by cold ambient temperatures.<sup>17,32</sup>

Average CO<sub>2</sub> emissions from vehicle DV at cold ambient temperatures and high altitude during the Alpine1 test ( $134 \pm 1 \text{ g km}^{-1}$ ) were comparable with those obtained from the RDE tests performed at 23 °C ( $134 \text{ g km}^{-1}$ ) and ~7% higher relative to 23 °C WLTP test emissions ( $125 \pm 5 \text{ g km}^{-1}$ ). Average CO<sub>2</sub> emissions were 7% higher on the more demanding Alpine2 (extra) route. CO<sub>2</sub> emissions from the urban section of on-road trips were 5%, 10%, and 3% lower for the RDE, Alpine1, and



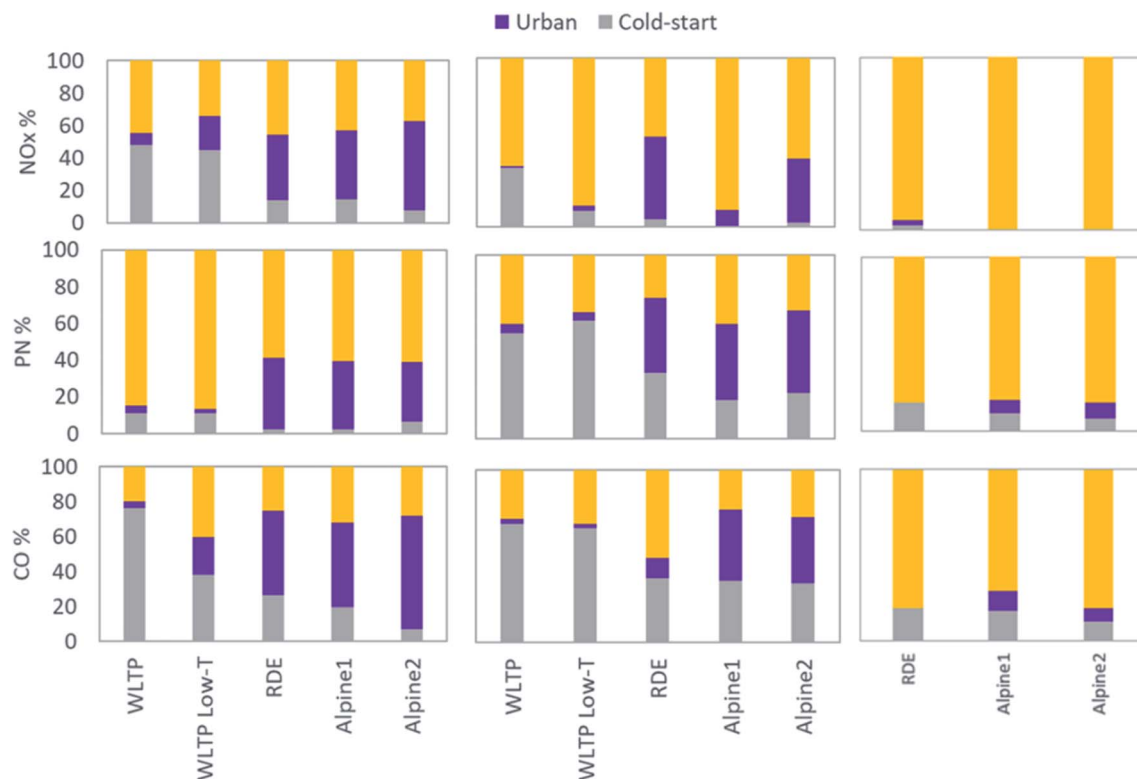


Fig. 5 Relative contribution (%) of cold-start emissions (grey) and those from the urban section of the on-road tests and low phase of the WLTP (violet) to the total emissions of NO<sub>x</sub>, PN and CO recorded during each test for the DV (left panels), the GV (central panels) and the PHEV (right panels).

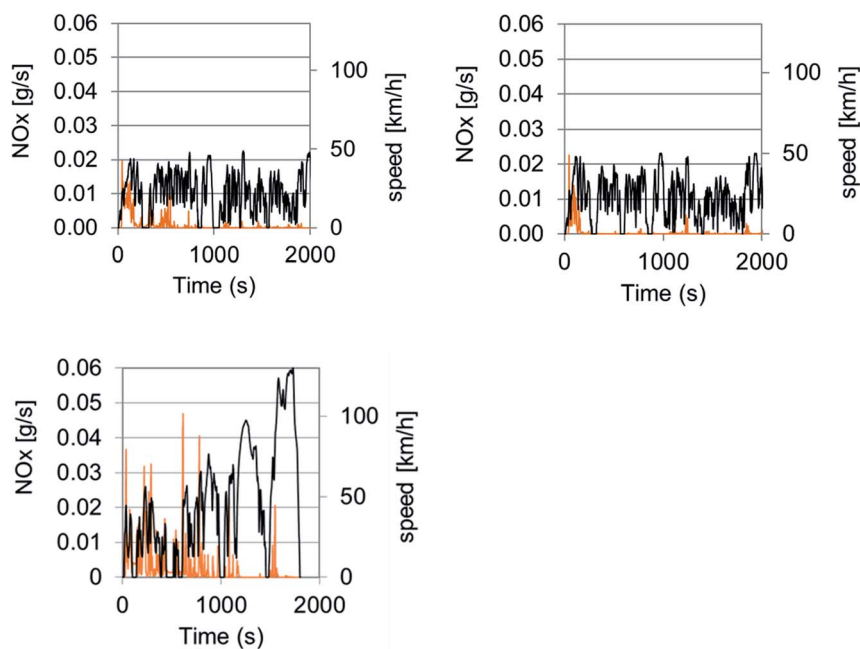


Fig. 6 NO<sub>x</sub> emission profiles of the DV during the first 2000 seconds of the two repetitions performed for route Alpine1. In the left panel, the coolant temperature was  $-2^{\circ}\text{C}$  at time 0 seconds, in the right panel it was at  $4^{\circ}\text{C}$ . The bottom panel is a test using the WLTC and coolant temperature at  $-7^{\circ}\text{C}$ . NO<sub>x</sub> emission profiles are presented with orange lines and the speed profiles with black lines.





Alpine2 routes, respectively, compared to the WLTP (low speed phase) 23 °C test results. The reason for the higher urban CO<sub>2</sub> emissions from the WLTP could be the much shorter distance driven in the low speed phase of the WLTP (10 times lower) compared to the distance driven on-road under urban conditions, and hence a higher impact of the cold-start CO<sub>2</sub> emissions on WLTP test results. When only cold-start CO<sub>2</sub> emissions are isolated (first 300 seconds of the trips), the CO<sub>2</sub> emissions of the on-road trips were 52%, 64%, and 150% higher for the RDE, Alpine1, and Alpine2 routes, respectively, compared to the WLTP 23 °C test, and 13%, 22%, and 86%, respectively, compared to the WLTP −7 °C test results, underlining the very challenging start of the Alpine2 route.

### 3.2. Emissions from the Euro 6d-TEMP gasoline vehicle (GV)

NOx emissions from the GV were below the Euro 6d-TEMP on-road requirements during the RDE tests. These emissions were overall higher during the tests performed at sub-zero temperatures than at those performed above 0 °C, especially on the Alpine routes, performed between −8 and −5 °C (Fig. 2).§

Higher NOx emissions at colder ambient temperatures in gasoline vehicles could be caused by a delayed light-off of the TWC.<sup>17,19,37,38</sup> Fig. S3 of the ESI† reports cumulative NOx and CO emissions for Alpine1, Alpine 2(extra) and RDE1 routes. By comparing the profiles, it seems that CO is well controlled from the beginning besides the initial sudden increase related to cold-start, demonstrating that the TWC is fully functional. In addition, the bulk of NOx emission is concentrated in later stages of the cycle, indicating that the delayed light-off seems to play a minor role in this situation. Overall, cold-start NOx emissions during all cold and on-road tests were low (less than 9% of the total emissions, see Fig. 5), indicating that, for this vehicle, the cold temperature, high altitude and road grade did not have a strong impact on NOx emissions (Fig. 3 and 5). However, as discussed later, this is not the case for CO emissions, as cold-start emissions accounted for 35–66% of the total CO emissions. This again indicated that cold-start is not always the main source of emissions for all criteria emissions as often suggested for gasoline vehicles.

While NOx emissions during the complete WLTP were higher at cold temperature ( $69 \pm 22 \text{ mg km}^{-1}$ ) than at 23 °C ( $36 \pm 1 \text{ mg km}^{-1}$ ), during cold-start and the urban section of the WLTP (low phase), emissions were lower at −7 °C than at 23 °C (see Fig. 3). This underlines the importance of the contribution from all phases of the cycle, also after catalyst light-off. It is worth noting that, while cold-start NOx emissions from Euro 3 and Euro 4 gasoline vehicles equipped with TWC did not seem to be sensitive to temperature changes,<sup>18</sup> a change in this trend was reported for Euro 5 and Euro 6b vehicles, with Euro 6b

gasoline vehicles emitting more NOx than Euro 5.<sup>17,18,38</sup> The results obtained for the GV suggest that temperature sensitivity may be dependent on the engine/catalyst/calibration strategy.

Urban NOx emissions on the Alpine2 (extra) route ( $170 \pm 82 \text{ mg km}^{-1}$ ), which starts with a high positive road grade (698 m of positive cumulative altitude gain over the first 9.2 km; see Fig. 1), were several times higher than during the urban sections of RDE compliant routes ( $52 \pm 8 \text{ mg km}^{-1}$ ) and Alpine1 ( $44 \pm 10 \text{ mg km}^{-1}$ ), which exhibit a lower road grade, as also shown in Fig. S3 of the ESI.† This suggests that road grade (and possibly its combination with very high altitude) may have had a strong impact on the NOx emissions of this vehicle. Indeed, as reported in Table S2 of the ESI,† CO<sub>2</sub> emissions during the cold start phase on the Alpine2 (extra) route were significantly higher when compared to RDE compliant routes ( $322 \pm 12 \text{ g km}^{-1}$  vs.  $200 \pm 5 \text{ g km}^{-1}$ ), possibly indicating an increased power demand to the engine. The high NOx emissions and the air-to-fuel ratios recorded indicate that the vehicle was using a lean combustion strategy during the high NOx events (see Fig. S4 of the ESI†). As a result, on the Alpine tests the GV presented NOx emissions that were up to 2.4 times higher than those measured from the DV.

Weber *et al.*<sup>15</sup> recently hypothesised for a series of gasoline vehicles tested over the NEDC that sharp NOx emission spikes correlating with increased power demand in the driving cycle are caused by lean mode engine operation to fulfil the higher power demand. Non-stoichiometric engine control drives the balance of the pollutants that are emitted. While lean operation results in high emissions of NO and low emissions of CO, rich operation results in high emissions of CO and low emissions of NOx. In the case of the GV, the low CO emissions measured also support the idea of lean engine operation.

CO emissions from vehicle GV were very low ( $<155 \text{ mg km}^{-1}$ ) throughout the tests, with the only exception of the WLTP test at −7 °C ( $659 \pm 96 \text{ mg km}^{-1}$ ; Euro 6 limit is  $1000 \text{ mg km}^{-1}$  for the 23 °C test). About 35% of the CO emissions measured during the 79–94 km on road tests took place within the first 300 seconds (as we have defined the cold-start), before the TWC reached its light-off temperature and about 70% in the urban section of the tests. As a consequence, the CO cold-start emissions factors during the on-road tests ranged from  $1687 \pm 605 \text{ mg km}^{-1}$  during the Alpine2 test (extra) (−6 °C) to  $1909 \pm 1399 \text{ mg km}^{-1}$  and  $2119 \pm 1054 \text{ mg km}^{-1}$  on RDE and Alpine1 routes, respectively.

During the cold-start of RDE routes, the average ambient temperature was 13 °C, which suggests that cold ambient temperature did not significantly affect the catalyst performance during the tests. However, during the laboratory tests, cold-start emissions of CO were five times higher at −7 °C than at 23 °C. While on-road CO emissions were lower than those measured for a series of Euro 6b vehicles tested using the WLTP at −7 °C, the emission factor obtained in the laboratory was in line with those of the Euro 6b gasoline vehicles.<sup>17,41</sup>

PN emissions for vehicle GV were sufficiently well controlled ( $<6 \times 10^{11} \text{ \# per km}$ ) during most tests ( $7 \text{ to } 9 \times 10^{11} \text{ \# per km}$  on the RDE and Alpine1 routes and during the WLTP at 23 °C), but increased by an order of magnitude during the WLTP tests at −7

§ At the time of the testing, this vehicle model exhibited unusually high emissions of NOx under motorway driving conditions. This emission behaviour was investigated by the European Commission in collaboration with the authorities. In spring 2019, the vehicle manufacturer identified a problem with the calibration of the lambda sensor that was leading to higher than expected NOx emissions and launched a recall to fix the problem. A detailed explanation of the case can be found in Clairotte *et al.*, 2020 (Chapter 5.1.1).<sup>39</sup>



°C ( $3.2 \times 10^{12}$  # per km) and on the Alpine2 (extra) route ( $1.4 \times 10^{12}$  # per km). The highest PN emission factors were found in the urban section for all types of tests (on-road tests and WLTP), ranging from  $7 \times 10^{11}$  # per km during one Alpine1 test to  $1.8 \times 10^{13}$  # per km during the WLTP at  $-7$  °C. Extremely high PN cold-start emission factors (up to  $1.6 \times 10^{13}$  # per km during Alpine2 (extra) and  $2.5 \times 10^{13}$  # per km during the WLTP at  $-7$  °C) were obtained (Fig. 3). The PN emission factor from the Alpine2 (extra) route, the most severe of the tests performed, was comparable to those reported in a previous study<sup>17</sup> for a Euro 6b PFI tested using the WLTP at  $-7$  °C. Emissions on the Alpine1 route were two times lower than those of the Euro 6b PFI vehicle. Previous studies have shown high PN emissions from gasoline vehicles using PFI engines tested in the laboratory at cold ambient temperatures.<sup>17,40,41</sup> Such high PN emissions from PFI vehicles at cold temperature are linked to enrichment of the air-fuel mixture during cold-start engine operation, which compensates for the reduced fuel vaporization and elevated friction of engine components, leading to incomplete fuel combustion.<sup>42</sup>

CO<sub>2</sub> emission factors during the Alpine tests ( $150 \pm 2$  g km<sup>-1</sup> and  $152 \pm 5$  g km<sup>-1</sup>) were comparable to the tests performed along the RDE-compliant routes ( $149 \pm 0$  g km<sup>-1</sup>) and 18–21% higher relative to 23 °C WLTP test emissions ( $126 \pm 0$  g km<sup>-1</sup>). CO<sub>2</sub> emissions during the WLTP were 12% higher at  $-7$  °C than at 23 °C. This is in agreement with previous laboratory studies performed on Euro 6b PFI vehicles using the WLTP, that confirmed an ~16% increase in CO<sub>2</sub> emissions as the temperature decreased from 23 °C to  $-7$  °C.<sup>17,40</sup> Unlike the diesel vehicle, this gasoline vehicle had higher on-road urban CO<sub>2</sub>

emissions (9–15% higher) compared to CO<sub>2</sub> emissions from the WLTP's low speed phase, despite a longer trip duration and lower impact of the cold start effect relative to the WLTP test. These results confirm that low-powered gasoline PFI engines have higher fuel consumption (and, accordingly, higher CO<sub>2</sub> emissions) under these low-temperature, more dynamic and transient conditions compared to diesel vehicles, and therefore, higher deviation from WLTP test results.

### 3.3. Emissions from the Euro 6d-TEMP gasoline plug-in hybrid vehicle (PHEV)

The vehicle PHEV exhibited relatively low emissions during most of the conditions tested, with the exception of the PN emissions that were high under some operations and CO emissions during the WLTP cold test (see Fig. 2, 7, Tables S4 and S5 of the ESI†). The emissions during the urban section were lower than those of the complete test because the vehicle operated in electric mode for up 99% of the section (in this case battery fully charged and cabin heating disabled; see Fig. 8). However, similarly to vehicle GV, CO and PN cold-start emission factors were often one order of magnitude higher than those measured during the entire on-road tests or the urban section (Fig. 3). The highest cold-start emissions were measured for the Alpine1 and the WLTP Low-T tests. These were the tests performed at the lowest ambient temperature and that started with the coldest engine/coolant temperature. This highlights the important contribution of these short events and the strong impact that temperature has on the emissions.<sup>45</sup>

NOx emissions from vehicle PHEV were very low (<6 mg km<sup>-1</sup>) under most of the studied routes (maximum emissions

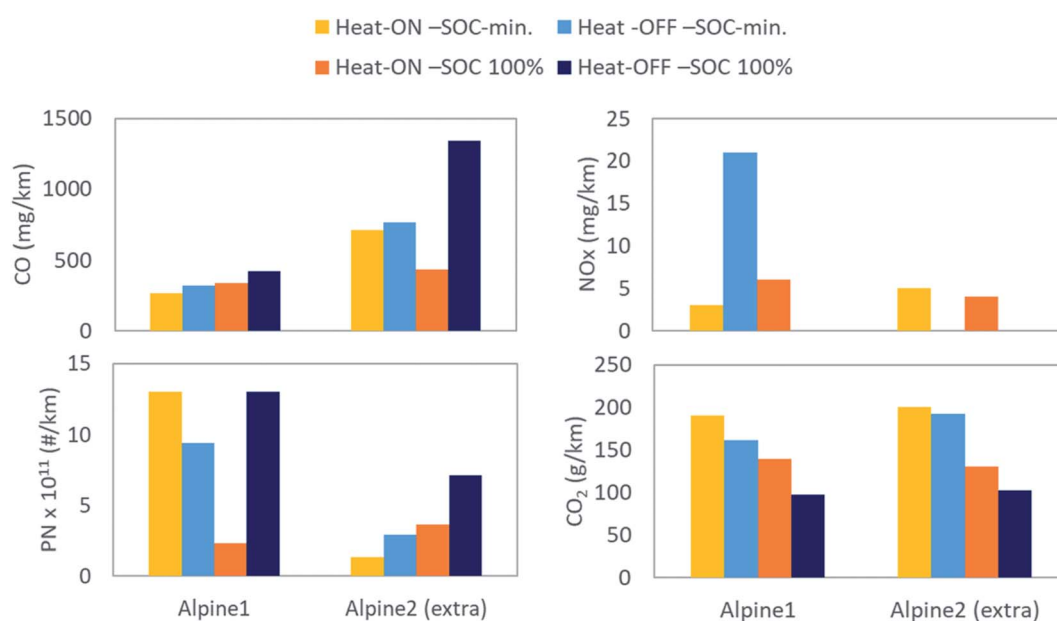
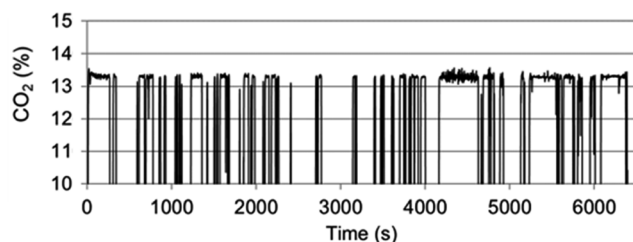


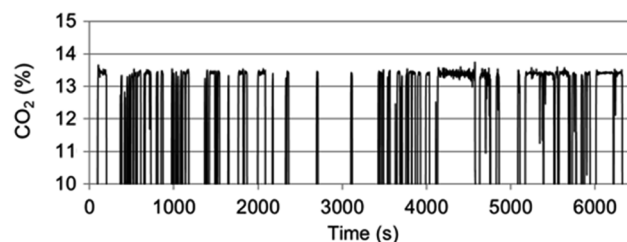
Fig. 7 Emission factors of PHEV for NOx, CO, PN, and CO<sub>2</sub>, corresponding to the complete on-road tests during the Alpine1 and Alpine2 (extra) tests. All tests were performed with the PHEV at depleted battery (SOC-min) and 100% battery SOC and with the air conditioning heating system enabled (Heat-ON) and disabled (Heat-OFF). Coolant temperature ranged between 4 °C and 8 °C. Emissions factors for the test Alpine1 – Heat-OFF – SOC-min (light blue bars) were calculated by correcting a shift on the exhaust flow rate and multiplying it by a 3.7 factor. Therefore, the values should be taken as indicative.



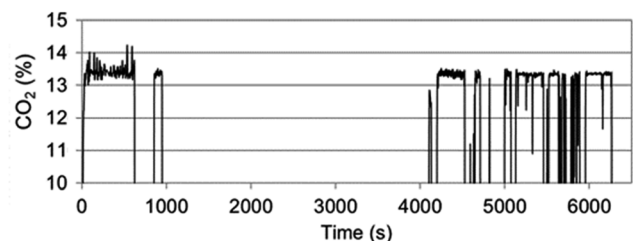
Alpine1 – SOC-min. – Heat-ON



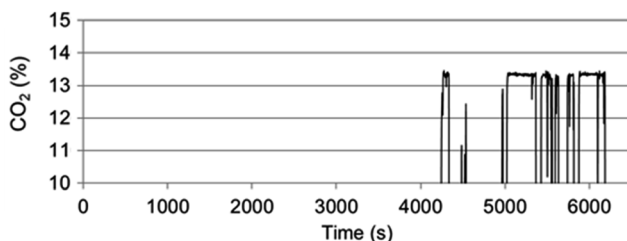
Alpine1 – SOC-min. – Heat-OFF



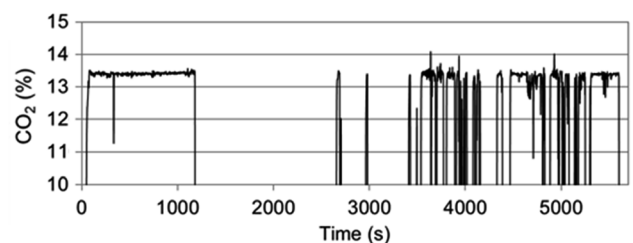
Alpine1 – SOC 100% – Heat-ON



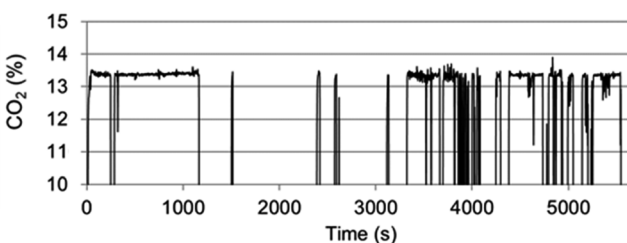
Alpine1 – SOC 100% – Heat-OFF



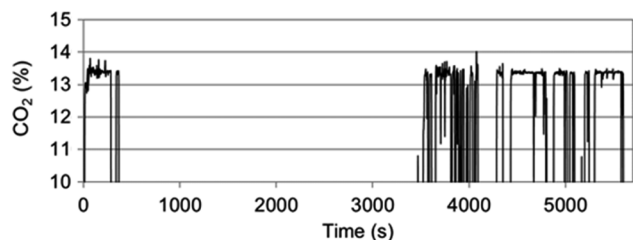
Alpine2 (extra) – SOC-min. – Heat-ON



Alpine2 (extra) – SOC-min. – Heat-OFF



Alpine2 (extra) – SOC 100% – Heat-ON



Alpine2 (extra) – SOC 100% – Heat-OFF

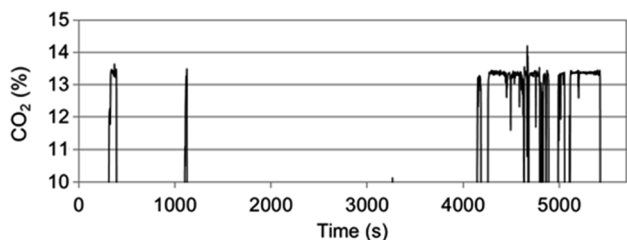


Fig. 8 CO<sub>2</sub> emission profile during the Alpine1 and Alpine2 (extra) tests performed with vehicle PHEV at 100% battery SOC and at depleted battery (SOC-min) and with the heating system enabled (Heat-ON) and disabled (Heat-OFF). CO<sub>2</sub> emissions are an indicator of the ICE operation.

of 18 mg km<sup>-1</sup> on the rural section of the Alpine2 (extra) route). NO<sub>x</sub> emissions were comparable during the RDE-compliant route tests performed at 8 °C (4 to 7 mg km<sup>-1</sup>) and the Alpine route tests performed at -4 °C to -1 °C (up to 7 mg km<sup>-1</sup>), which indicates that cold temperature and high altitudes beyond the RDE boundary condition of 1300 m.a.s.l. did not affect these emissions. Cold-start emissions for this vehicle were ~10 mg km<sup>-1</sup> to up to 140 mg km<sup>-1</sup> lower than those of vehicle GV (the other gasoline vehicle under test).

NO<sub>x</sub> emissions are comparable to those reported from a Euro 5 plug-in hybrid tested at -7 °C on the WLTC (5 ± 2 mg km<sup>-1</sup>).<sup>43</sup> However, we observed that the NO<sub>x</sub>/CO trade-off discussed above for the GV is towards the emissions of CO. In fact, even if part of the routes were covered by the pure electric mode, the CO emissions from the PHEV were the highest of all three vehicles tested (up to 1343 mg km<sup>-1</sup> for Alpine2 (extra) Heat-OFF 100% SOC) suggesting fuel-rich operation.



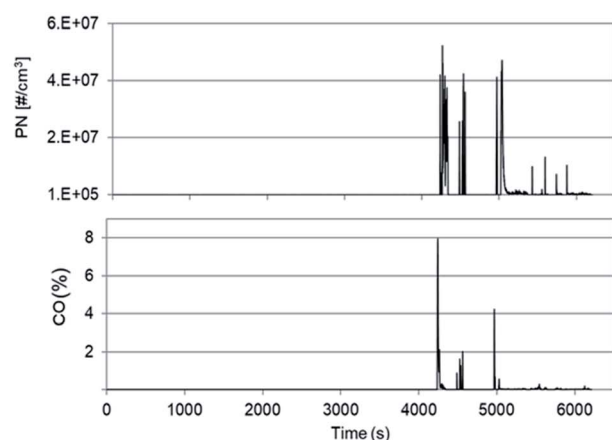
The use of the vehicle PHEV's heating system had a significant effect on the use of the ICE of the vehicle and consequently its emissions. During Alpine1 and Alpine2 (extra) tests, where temperature was below  $-1^{\circ}\text{C}$ , and whenever the heating system was activated, the ICE started as soon as the test initiated (see Fig. 8 where the  $\text{CO}_2$  emission profile corresponds to ICE use). This resulted in an  $\sim 30\%$  increase of  $\text{CO}_2$  emissions for the tests performed with the battery fully charged (SOC 100%).

CO and PN cold-start emissions during the Alpine tests (SOC 100% – Heat-ON) accounted for 7–18% of the total emissions. After 400–1000 s of ICE operation, the electric operation begins and goes on for the entire urban section. Then, once the rural starts and the vehicle travels at more than  $\sim 75\text{ km h}^{-1}$  the ICE ignites again resulting in a second cold-start event, this time at higher engine load, which in turn results in higher CO and PN emissions than the first one (Fig. 9). This behavior was already shown by Yang *et al.* for hybrid vehicles and also resulted in high PN emissions.<sup>46</sup>

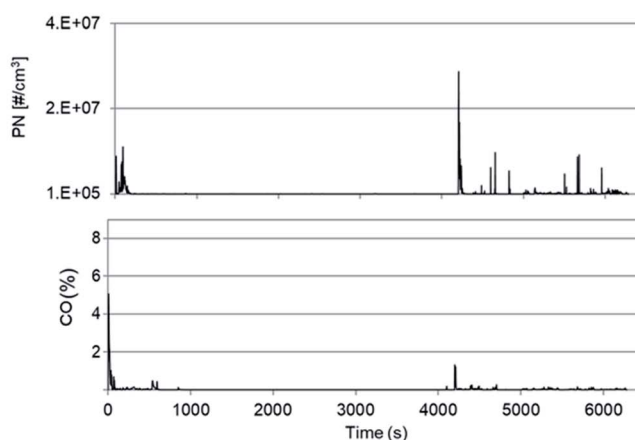
On the Alpine routes and when the vehicle was fully charged (SOC 100%), CO and/or PN emissions were higher when the

heating system was disabled (OFF) than when it was enabled (ON) (Fig. 7). A similar impact of Heat-OFF and Heat-ON states on the CO and PN emissions (and also THC emissions) during charge depleting operation was also reported for two plug-in hybrid vehicles tested over the WLTP at  $-7^{\circ}\text{C}$ .<sup>32</sup> The study shows that the higher emissions during the Heat-OFF tests compared to the Heat-ON tests may be linked to the way that the engine and TWC are heated during the two different operation modes. As illustrated by the emission rates presented in Fig. S5 of the ESI,<sup>†</sup> when the heating system is enabled (or the initial SOC is low), the ICE is more likely to start while the vehicle is stopped, which allows for the engine and TWC to heat up in a more controlled manner during low-speed/low-load operation typical of the start of a trip. On the other hand, when the heating system is disabled, the ICE is more likely to start at higher loads, while the vehicle is already running. The combination of the high load and cold engine/catalyst may result in incomplete combustion of the fuel, *i.e.*, high emissions of particles and CO, showing that a catalyst that has not reached light-off is not capable of performing oxidation.

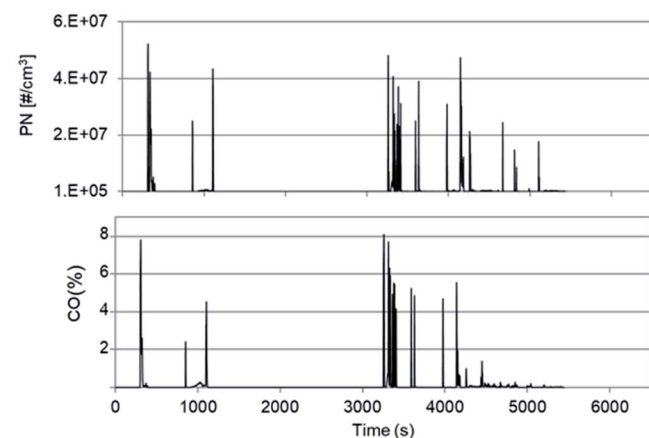
Alpine1– SOC 100% – Heat-OFF



Alpine1– SOC 100% – Heat-ON



Alpine2 (extra) – SOC 100% – Heat-OFF



Alpine2 (extra) – SOC 100% – Heat-ON

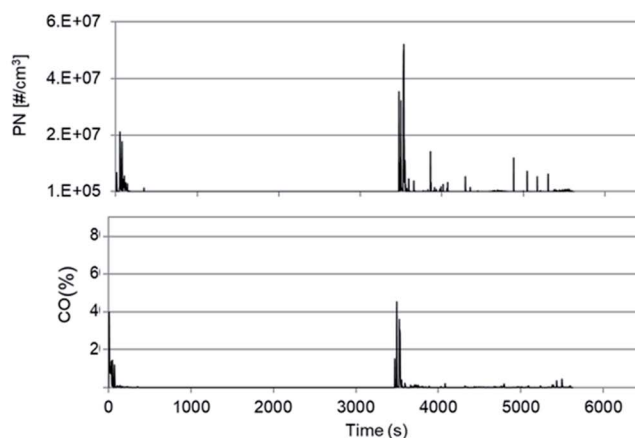


Fig. 9 Vehicle PHEV emission profiles of CO and PN on the Alpine routes at 100% SOC (Alpine1 top panels; Alpine2 (extra) bottom panels) with the heating system disabled (left panels) and with the heating system enabled (right panels).





CO and PN emissions do not correlate with CO<sub>2</sub> emission factors and electric vehicle operation. For instance, while the CO<sub>2</sub> emission factor during the test Alpine2 (extra) – Heat-ON – SOC-min was 201 g km<sup>-1</sup>, CO was 713 mg km<sup>-1</sup> and PN was  $1.3 \times 10^{11}$  # per km, the CO<sub>2</sub> emission factor during the test Alpine2 (extra) – Heat-OFF – SOC 100% was 102 g km<sup>-1</sup>, CO was 1343 mg km<sup>-1</sup> and PN was  $7.1 \times 10^{11}$  # per km. This suggests that the emissions of CO and PN can be driven by cold-start behavior, which for this PHEV vehicle is in turn likely influenced by the combination of the thermal state of the aftertreatment systems, SOC and driving situation at ICE start.

CO<sub>2</sub> emissions, on the same route and with a 100% SOC, were 27–43% higher when the heating system was enabled than when it was disabled. CO<sub>2</sub> emissions from the routes where vehicles were driven with a fully charged battery at start (100% SOC) were 68–148% higher compared to utility factor weighed CO<sub>2</sub> emissions from the WLTP test done at 23 °C and 25–85% higher compared to utility factor weighed CO<sub>2</sub> emissions from the WLTP test done at –7 °C. For the case Heat-OFF – SOC 100%, CO<sub>2</sub> emissions were also comparable to those on the RDE1 route that was within the RDE boundary conditions of temperature and altitude. As expected, CO<sub>2</sub> emissions were also higher (37–67% relative to tests with the battery fully charged at start) for the routes where the vehicle was driven in charge-sustaining mode with a depleted battery at the start of the test. Besides its larger engine capacity and weight, the CO<sub>2</sub> emissions from the PHEV were 47% to 56% lower than those measured from DV and GV during the WLTP tests at the two studied temperatures. However, this difference is largely reduced during on-road tests with a fully charged battery, where the CO<sub>2</sub> emissions from the PHEV were 11% and 20% lower than those from the DV and GV on the RDE routes and from comparable to 14% lower during the Alpine tests.

## 4. Conclusions

The on-road emissions of NO<sub>x</sub>, CO, PN and CO<sub>2</sub> from three Euro 6d-TEMP certified passenger cars—one diesel, one gasoline, and one gasoline plug-in hybrid electric vehicle—were investigated under a broad range of conditions, including conventional RDE-compliant tests and also demanding tests on mountain roads with sub-zero ambient temperatures, high road grade and high altitudes. Laboratory testing was also conducted using the WLTP cycle at 23 °C and –7 °C.

Our results indicate that CO, NO<sub>x</sub> and PN emissions from the studied Euro 6d-TEMP certified vehicles were higher at colder temperatures during both laboratory and on-road tests. Emissions were predictably higher for the tests performed on the most demanding route (Alpine2 (extra)) that, besides the cold ambient temperature, reached 2000 m.a.s.l. and had a high road grade segment at the beginning of the urban section (698 m of positive gain over the first 9.2 km; see Fig. 1).

Although CO, NO<sub>x</sub> and PN emissions were higher at colder temperature and higher altitudes, the raw emissions during on-road tests were below Euro 6d-TEMP on-road emission requirements for the complete and the urban sections. With the exception of the urban NO<sub>x</sub> emissions from DV and GV during

one of the two tests performed with each vehicle on the demanding Alpine2 (extra) route, ‘raw’ emission levels were below Euro 6d-TEMP on-road emission requirements, even if they were not divided by the 1.6 factor applicable during the extended conditions of the RDE test. This is an encouraging sign of the ability of RDE-compliant Euro 6d-TEMP vehicles to deliver consistently lower emissions than pre-RDE vehicles, even under very demanding driving conditions. Nonetheless, the high emissions of different pollutants during cold-start, the high PN emissions of GV and the high PN emissions of PHEV under certain operations, indicate there is still room for improvement. Particular attention should be paid to the emissions during cold-start due to their particular impact on urban air quality.

The use of the cabin air heating system in the PHEV had a significant effect on the use of the ICE of the vehicle, and consequently on its emissions. Although NO<sub>x</sub> emissions (up to 21 mg km<sup>-1</sup>) from vehicle PHEV were low under all the studied conditions, CO (up to 1343 mg km<sup>-1</sup>) and PN (up to  $1.3 \times 10^{12}$  # per km) emissions were high in some of the scenarios studied.

Our results indicate that, following the introduction of the RDE emissions testing procedure in the EU, more efficient emission control technologies and strategies are being used to reduce the emissions of the pollutants from vehicles covered by this test procedure, both within and beyond the boundary conditions set by it. This is particularly true for NO<sub>x</sub> emissions from diesel vehicles. However, pollutant emissions from certain vehicle technologies that are not currently regulated by the Euro 6 regulation were measured at very high levels in some cases. These emissions were often concentrated in the cold-start phase, and associated with specific combinations of initial battery SOC, low ambient temperatures and driving situations at ICE start (especially for the PHEV vehicle). An improvement of the emissions performance of new vehicles under such situations could be addressed by expanding the boundary conditions of the RDE test and by setting technology-neutral emission limits that apply equally, regardless of vehicle technology.

## Disclaimer

The opinions expressed in this manuscript are those of the authors and should not be considered to represent an official position of the European Commission.

## Conflicts of interest

There are no conflicts to declare.

## Acknowledgements

The authors would like to acknowledge the support and collaboration of A. Bonamin, F. Buchet, M. Cadario, M. Carrero, G. Cotogno, F. Forloni, F. Forni, P. Le Lijour, D. Lesueur, F. Montigny, V. Padovan, M. Sculati, M. Otura-Garcia and A. Zappia.



## References

- European Environmental Agency, *Air quality in Europe—2018 report*, EEA Report No 12/2018, ISBN 978-92-9213-989-6, ISSN 1977-8449, DOI: 10.2800/777411.
- D. Custódio, M. Cerqueira, C. Alvesa, T. Nunes, C. Pio, V. Esteves, D. Frosini, F. Lucarelli and X. Querole, *Sci. Total Environ.*, 2016, **562**, 822–833.
- Q. Wang, N. Jiang, S. Yin, X. Li, F. Yu, Y. Guo and R. Zhang, Carbonaceous species in PM<sub>2.5</sub> and PM<sub>10</sub> in urban area of Zhengzhou in China: seasonal variations and source apportionment, *Atmos. Res.*, 2017, **191**, 1–11.
- L. Xing, J. Wu, M. Elser, S. Tong, S. Liu, X. Li, L. Liu, J. Cao, J. Zhou, I. El-Haddad, R. Huang, M. Ge, X. Tie, A. S. H. Prévôt and G. Li, *Atmos. Chem. Phys.*, 2019, **19**, 2343–2359.
- J. Hofman, J. Staelens, R. Cordell, C. Stroobants, N. Zikova, S. M. L. Hama, K. P. Wyche, G. P. A. Kos, S. V. D. Zee, K. L. Smallbone, E. P. Weijers, P. S. Monks and E. Roekens, *Atmos. Environ.*, 2016, **136**, 68–81.
- S. M. L. Hama, R. L. Cordella and P. S. Monks, *Atmos. Environ.*, 2017, **166**, 62–78.
- T. D. Gordon, A. A. Presto, N. T. Nguyen, W. H. Robertson, K. Na, K. N. Sahay, M. Zhang, C. Maddox, P. Rieger, S. Chattopadhyay, H. Maldonado, M. M. Maricq and A. L. Robinson, *Atmos. Chem. Phys.*, 2014, **14**, 4643–4659.
- S. M. Platt, I. El Haddad, S. M. Pieber, A. A. Zardini, R. Suarez-Bertoa, M. Clairotte, K. R. Daellenbach, R. J. Huang, J. G. Slowik, S. Hellebust, B. Temime-Roussel, N. Marchand, J. de Gouw, J. L. Jimenez, P. L. Hayes, A. L. Robinson, U. Baltensperger, C. Astorga and A. S. H. Prévôt, *Sci. Rep.*, 2017, **7**, 4926.
- R. Suarez-Bertoa, A. A. Zardini, S. M. Platt, S. Hellebust, S. M. Pieber, I. El Haddad, B. Temime-Roussel, U. Baltensperger, N. Marchand, A. S. H. Prévôt and C. Astorga, *Atmos. Environ.*, 2015, **117**, 200–211.
- M. F. Link, J. Kim, G. Park, T. Lee, T. Park, Z. B. Babar, K. Sung, P. Kim, S. Kang, J. S. Kim, Y. Choi, J. Son, H.-J. Lim and D. K. Farmer, *Atmos. Environ.*, 2017, **156**, 95–101.
- S. C. Anenberg, J. Miller, R. Minjares, L. Du, D. K. Henze, F. Lacey, C. S. Malley, L. Emberson, V. Franco, Z. Klimont and C. Heyes, *Nature*, 2017, **545**, 467–471.
- C. Giorio, A. Tapparo, M. Dall'Osto, D. C. S. Beddows, J. K. Esser-Gietl, R. M. Healy and R. M. Harrison, *Environ. Sci. Technol.*, 2015, **49**, 3330–3340.
- J. Pey, N. Pérez, X. Querol, A. Alastuey, M. Cusack and C. Reche, *Sci. Total Environ.*, 2010, **408**, 1951–1959.
- S. M. Platt, I. E. Haddad, S. M. Pieber, R.-J. Huang, A. A. Zardini, M. Clairotte, R. Suarez-Bertoa, P. Barmet, L. Pfaffenberger, R. Wolf, J. G. Slowik, S. J. Fuller, M. Kalberer, R. Chirico, J. Dommen, C. Astorga, R. Zimmermann, N. Marchand, S. Hellebust, B. Temime-Roussel, U. Baltensperger and A. S. H. Prévôt, *Nat. Commun.*, 2014, **5**, 3749.
- C. Weber, I. Sundvor and E. Figenbaum, *Atmos. Environ.*, 2019, **206**, 208–217.
- R. Suarez-Bertoa and C. Astorga, *Atmos. Environ.*, 2016, **136**, 134–143.
- R. Suarez-Bertoa and C. Astorga, *Environ. Pollut.*, 2018, **234**, 318–329.
- M. Weilenmann, P. Soltic, C. Saxer, A.-M. Forss and N. Heeb, *Atmos. Environ.*, 2005, **39**, 2433–2441.
- M. Clairotte, T. W. Adam, A. A. Zardini, U. Manfredi, G. Martini, A. Krasenbrink, A. Vicet, E. Tournié and C. Astorga, *Appl. Energy*, 2013, **102**, 44–54.
- H. Wang, Y. Ge, L. Hao, X. Xu, J. Tan, J. Li, L. Wu, J. Yang, D. Yang, J. Peng, J. Yang and R. Yang, *Atmos. Environ.*, 2018, **191**, 126–131.
- H. Wang, H. Yin, Y. S. Ge, L. Yu, Z. Xu, C. Yu, X. Shi and H. Liu, *Atmos. Environ.*, 2013, **81**, 263–269.
- A. Nagpure, B. Gurjar and P. Kumar, *Atmos. Environ.*, 2011, **45**, 1413–1417.
- European Commission, *Commission regulation (EU) 2018/1832*, Official Journal of the European Union, 301, 27.11.2018, 1–314, 2018.
- Y. Wu, S. Zhang, J. Hao, H. Liu, X. Wu, J. Hu, M. P. Walsh, T. J. Wallington, K. M. Zhang and S. Stevanovic, *Sci. Total Environ.*, 2017, **574**, 332–349.
- H. Dinodia, N. Mahajan, V. Dwivedi and V. Khanna, *SAE Technical Paper*, 2018-01-0339, 2018, DOI: 10.4271/2018-01-0339.
- European Commission, *Commission regulation (EU) 2017/1151*, Official Journal of the European Union, L 175/1, 2017.
- European Commission, *Commission regulation (EU) 2017/1154*, Official Journal of the European Union, L 175/708, 2017.
- V. Valverde Morales and P. Bonnel, *On-road testing with Portable Emissions Measurement Systems (PEMS) - Guidance note for light-duty vehicles*, Publications Office of the European Union, 2018, DOI: 10.2760/08294, ISSN: 1831–9424.
- L. Ntziachristos, D. Gkatzoflias, C. Kouridis and Z. Samaras, *Information Technologies in Environmental Engineering*, 2009, pp. 491–504, DOI: 10.1007/978-3-540-88351-7\_37.
- UNECE Regulation 83, Official Journal of the European Union, L 42/1, 2012.
- UNECE GTR No. 15. UN Global Technical Regulation concerning the Worldwide harmonized Light vehicles Test Procedure (WLTP), Amendment 5, 2019, <https://www.unece.org/fileadmin/DAM/trans/main/wp29/wp29wgs/wp29gen/wp29registry/ECE-TRANS-180a15am5e.pdf>.
- R. Suarez-Bertoa, J. Pavlovic, G. Trentadue, M. Otura-Garcia, A. Tansini, B. Ciuffo and C. Astorga, *ACS Omega*, 2019, **4**, 3159–3168.
- A. Ramos, J. Muñoz, F. Andrés and O. Armas, *Transp. Res. D: Trans. Environ.*, 2018, **63**, 37–48.
- B. Guan, R. Zhan, H. Lin and Z. Huang, *Appl. Therm. Eng.*, 2014, **66**, 395–414.
- M. Weiss, E. Paffumi, M. Clairotte, Y. Drossinos, T. Vlachos, P. Bonnel and B. Giechaskiel, *Including cold-start emissions in the Real-Driving Emissions (RDE) test procedure*, Publications Office of the European Union, 2017, DOI: 10.2760/70237.



- 36 V. Valverde Morales, M. Clairotte, J. Pavlovic, B. Giechaskiel and P. Bonnel, *SAE Technical Paper*, 2020-01-2219, 2020.
- 37 A. Roberts, R. Brooks and P. Shipway, *Energy Convers. Manage.*, 2014, **82**, 327–350.
- 38 C. Dardiotis, G. Martini, A. Marotta and U. Manfredi, *Appl. Energy*, 2013, **111**, 468–478.
- 39 M. Clairotte, V. Valverde, P. Bonnel, C. Gruening, J. Pavlovic, D. Manara, R. Loos, B. Giechaskiel, M. Carriero, M. Otura, R. Suarez-Bertoa, G. Martini and A. Krasenbrink, *Joint Research Centre 2019 Light-Duty Vehicles emissions testing*, Publications Office of the European Union, 2020, DOI: 10.2760/90664.
- 40 R. Zhu, J. Hu, X. Bao, L. He, L. Lai, L. Zu, Y. Li and S. Su, *Environ. Pollut.*, 2016, **216**, 223–234.
- 41 V. Valverde, B. Adrià Mora, M. Clairotte, J. Pavlovic, R. Suarez-Bertoa, B. Giechaskiel, C. Astorga-Llorens and G. Fontaras, *Atmosphere*, 2019, **10**, 243.
- 42 A. Joshi and T. Johnson, *Emiss. Control Sci. Technol.*, 2018, **4**, 219–239.
- 43 R. Suarez-Bertoa and C. Astorga, *Transp. Res. D: Trans. Environ.*, 2016, **49**, 259–270.
- 44 S. K. Grange, N. J. Farren, A. R. Vaughan, R. A. Rose and D. C. Carslaw, *Environ. Sci. Technol.*, 2019, **53**, 6587–6596.
- 45 A. Pham and M. Jetric, *SAE Technical Paper*, 2018-01-0428, 2018.
- 46 Z. Yang, Y. Ge, D. Thomas, X. Wang, S. Su, H. Li and H. H. Hongwen, *Atmos. Environ.*, 2019, **199**, 70–79.

